Since January 2020 Elsevier has created a COVID-19 resource centre with free information in English and Mandarin on the novel coronavirus COVID-19. The COVID-19 resource centre is hosted on Elsevier Connect, the company's public news and information website.

Virus Research 145 (2009) 260–269

Contents lists available at ScienceDirect

Virus Research

journal homepage: www.elsevier.com/locate/virusres

Elucidating the molecular physiopathology of acute respiratory distress syndrome in severe acute respiratory syndrome patients

Say Li Kong[a], Paul Chui[b], Bing Lim[a,c,*], Manuel Salto-Tellez[d,**]

[a] Genome Institute of Singapore, A*STAR (Agency for Science, Technology and Research), 60 Biopolis Street, Genome, #02-01, Singapore 138672, Singapore
[b] Health Sciences Authority, Centre for Forensic Medicine, 11 Outram Road, Singapore 169078, Singapore
[c] Harvard Institute of Medicine, 77 Ave Louis Pasteur, Boston, MA 02115, USA
[d] National University Health System and National University of Singapore, 5 Lower Kent Ridge Road, Singapore 119074, Singapore

ARTICLE INFO

Article history:
Received 8 April 2009
Received in revised form 19 July 2009
Accepted 19 July 2009
Available online 25 July 2009

Keywords:
ARDS
SARS-CoV infection
Pathogenesis
Therapeutic interventions

ABSTRACT

Acute respiratory distress syndrome (ARDS) is a severe form of acute lung injury. It is a response to various diseases of variable etiology, including SARS-CoV infection. To date, a comprehensive study of the genomic physiopathology of ARDS (and SARS) is lacking, primarily due to the difficulty of finding suitable materials to study the disease process at a tissue level (instead of blood, sputa or swaps). Hereby we attempt to provide such study by analyzing autopsy lung samples from patient who died of SARS and showed different degrees of severity of the pulmonary involvement. We performed real-time quantitative PCR analysis of 107 genes with functional roles in inflammation, coagulation, fibrosis and apoptosis; some key genes were confirmed at a protein expression level by immunohistochemistry and correlated to the degree of morphological severity present in the individual samples analyzed. Significant expression levels were identified for ANPEP (a receptor for CoV), as well as inhibition of the STAT1 pathway, IFNs production and CXCL10 (a T-cell recruiter). Other genes unassociated to date with ARDS/SARS include C1Qb, C5R1, CASP3, CASP9, CD14, CD68, FGF7, HLA-DRA, IGF1, IRF3, MALAT-1, MSR1, NFIL3, SLPI, USP33, CLC, GBP1 and TAC1. As a result, we proposed to therapeutically target some of these genes with compounds such as ANPEP inhibitors, SLPI and dexamethasone. Ultimately, this study may serve as a model for future, tissue-based analyses of fibroinflammatory conditions affecting the lung.

1. Introduction

In 2003, the severe acute respiratory syndrome (SARS) emerged as a life-threatening disease that caused 8096 cases and 774 deaths in 29 countries (http://www.who.int, 2003). A new coronavirus (SARS-CoV) was identified as the causative pathogen (Ksiazek et al., 2003). It trigged fever, dry cough, pulmonary infiltrates, lymphopenia and thrombocytopenia with a mortality rate of 10%. Sporadic cases of SARS-CoV infections due to laboratory exposure were reported after the global outbreak ended. The mechanisms underlying SARS-CoV infections and clinical manifestation remain poorly understood. The high lethality of SARS and its enormous economic and social impacts have highlighted the importance of elucidating the pathogenesis of SARS-CoV infection.

Acute respiratory distress syndrome (ARDS) is the most severe form of acute lung injury with a mortality rate of 30–50%. It is associated with SARS-CoV infection and characterized by pulmonary oedema, accumulation of inflammatory cells and resulting severe hypoxia. ARDS can initiate the activation of local inflammatory mediators that eventually spill over into the general circulation and resulting a systemic inflammatory response (SIR) (Bhatia and Moochhala, 2004). As a consequence of SIR, an excessive cytokine-mediated systemic leukocytes activation will lead to the multiple organ dysfunction syndrome (MODS). Owing to the development of ARDS, SARS-CoV infected patients often suffered from MODS, thus explaining its high mortality. Therefore, it is crucial to elucidate the key inflammatory mediators in ARDS to characterize novel therapeutic targets ultimately aiming to stop or ameliorate the disease progression.

Due to the ease of availability, most studies (Reghunathan et al., 2005; Ng et al., 2004) applied peripheral blood, throat swab and sputum samples to study the expression and cytokine profiles of SARS-CoV infected patients. However, Glass et al. (2004) has reported that SARS viral RNA is localized in bronchial and bronchiolar epithelium; while Ding et al. (2004) has shown that highest viral load was found in lung tissue of SARS-CoV infected

* Corresponding author at: National University Health System and National University of Singapore, 5 Lower Kent Ridge Road, Singapore 119074.
** Corresponding author. Fax: +65 67780671.
E-mail addresses: limb1@gis.a-star.edu.sg (B. Lim), patmst@nus.edu.sg (M. Salto-Tellez).

0168-1702/$ – see front matter © 2009 Elsevier B.V. All rights reserved.
doi:10.1016/j.virusres.2009.07.014

patients. Therefore, we attempted to utilize the formalin-fixed, paraffin-embedded (FFPE) tissue samples from SARS-CoV infected patients obtained from clinical autopsy examination as our experimental material. This allowed us to study the molecular changes which occurred at the tissue level, achieving a larger biological relevance.

During the onset of the SARS-CoV epidemic, we hypothesized that the antiviral activation in response to SARS-CoV infections would be mediated by complex mechanisms, where cytokines, chemokines, macrophages and T-cells would be involved through various pathways (Salto-Tellez et al., 2005). In this study, we characterize the inflammatory mediators involved in the development of ARDS in SARS-CoV infected patients by investigating the gene expression profiles linked to the physiopathological changes occurring in the lung. We show 26 genes that are significantly up-regulated and 5 genes that are significantly down-regulated in the progression of the disease. These genes greatly improve the knowledge of the pathogenesis of SARS-CoV infections and contribute towards the development of therapeutic interventions for this fatal disease and perhaps, for ARDS as a whole.

2. Materials and methods

2.1. Materials

A total of 12 formalin-fixed paraffin-embedded (FFPE) lung tissues from seven patients who died of SARS with positive PCR were obtained from the Health Science Authority (Singapore) with approval from the competent Institutional Ethic's Review Board (DSRB Reference Code B/00/369). The clinical information for these patients is shown in Table 1. Two FFPE lung samples from cases with normal lung histology were included as normal control from cases in which the cause of death was totally unrelated to any lung pathology, directly or indirectly, and with no macroscopic or histologic lung disease in the lungs from which these samples were taken.

2.2. Pathological examination

Section of specimens were stained with haematoxylin and eosin (H&E), and examined under light microscopy (Fig. 1). Five of the seven patients had multiple tissues from different areas of the lung showing the disease at different grades of evolution. All these samples were representative of the spectrum of changes in ARDS, showing a clear disease progression from early stage leading to the end-stage lung fibrosis. The morphological description of these samples is shown in Table 2.

2.3. Sectioning of FFPE samples

Several sections from each FFPE sample were collected in an RNase-free environment with RNaseZap (Ambion Inc., TX) and used for RNA extraction (10 μm thick) and immunohistochemistry experiments (5 μm thick).

2.4. RNA extraction

Total RNA was isolated from sections of FFPE samples using the Paraffin Block RNA Isolation Kit (Ambion Inc., TX). The FFPE sections were incubated with xylene to remove the paraffin. The tissues were then digested with Proteinase K. The RNA was isolated using Acid Phenol Chloroform, followed by precipitation with isopropanol using linear acrylamide as carrier. DNase I treatment was included to eliminate contamination of genomic DNA.

2.5. Reverse-transcriptase PCR (RT-PCR)

RT-PCR from 1 μg of RNA template was performed using SuperScript III™ (Invitrogen, CA) to allow for better specificity and higher yields of full-length cDNA products. RNase H digestion was later introduced to remove the RNA templates from cDNA:RNA hybrid molecules for higher sensitivity.

2.6. Quantitative real-time PCR

We designed a Low Density TaqMan Array® (LDTA) on Micro Fluidic Card (Applied Biosystems, CA). Quantitative real-time PCR experiments were carried out with pre-developed TaqMan® probes and TaqMan® Universal PCR Master Mix in the ABI7900 Real-time PCR (Applied Biosystems, CA) system. All real-time PCR experiments were done in four replicate reactions. All real-time PCR results were expressed as fold changes in mRNA expression of patient samples with respect to the control samples. All results were normalized to the expression of the housekeeping gene β-actin in the PCR reactions.

2.7. Immunohistochemistry (IHC)

IHC for CD68, CD9, and PECAM-1 were performed according to the manufacturers' instructions. Briefly, FFPE sections were de-waxed and hydrated. After microwaving and blocking with endogenous peroxidase, the slides were incubated with the antibodies for CD68 (clone KP1, DAKO), CD9 (sc-13118, SANTA CRUZ), and PECAM-1 (clone JC70A, DAKO) stain for 1 h at room temperature, followed by incubation with Envision HRP detection reagent (DAKO ChemMate). Normal bone marrow sections were used as positive controls, showing a representation of all inflammatory cell types. Negative controls were prepared by replacing the primary antibody with Tris-buffered saline. Expression of individual antibodies in the tissue sections was semi-quantitatively scored by a pathologist looking at overall expression in all the morphologically discernible cell types in the section.

2.8. Statistical analysis

Mann–Whitney and SAM analysis were performed to identify genes that are significantly up- or down-regulated in the progression of disease. For Mann–Whitney analysis, a p-value of ≤ 0.05 was considered significant, while q-value of <5% was considered significant for SAM test. We applied Ingenuity® Pathway Analysis (Ingenuity Systems Inc., Redwood City, CA) to study the functional network and canonical pathway of the genes (mean expression ≥ 1.5).

3. Results

We characterized the disease severity of SARS-CoV infection in individual FFPE lung samples based on the histopathological features as described in Table 2. We grouped the FFPE samples to early (Grades 1–6) and late (Grades 7–11) disease stage, demonstrating a clear disease progression from early stage leading to the end-stage lung fibrosis. Due to the bacterial overgrowth observed in the histological section of Sample B, it was eliminated from our analysis.

Real-time PCR experiments were carried out to validate the expression levels for 107 genes (refer Supplementary 1) with functional roles in inflammation, coagulation, fibrosis and apoptosis (refer Fig. 2). We grouped the samples to early and late disease stage to compute the average expression level of individual genes. By doing so, we identified a list of 92 genes that were over-expressed

Table 1
Clinical information of patients died of SARS-CoV infection.

	Patient						
	I	II	III	IV	V	VI	VII
Age	67	43	38	64	50	29	39
Gender	Female	Male	Male	Male	Male	Female	Male
Symptoms	Fever, dry cough	Fever	Fever with mild myalgia and chills	Fever	Fever, dry cough, myalgia, malaise	Fever, malaise, shortness of breath, dry cough	Fever, dry cough
Diagnosis	Diffuse alveolar damage	Early phase diffuse alveolar damage	Diffuse pneumonia	Bilateral infiltrates, progressive sepsis	Multiorgan failure secondary to SARS	Developed sepsism, multiorgan failure, bleeding tendencies	Atypical Pneumonia; acute myocardial infarct; septic shock
Treatment	Died at home	Collapsed when admitted	Cortico-steroid given	No cortico-steroid given	Cortico-steroid given	Cortico-steroid given	Cortico-steroid given
Mechanical ventilation	No	No	Yes	Yes	Yes	Yes	Yes

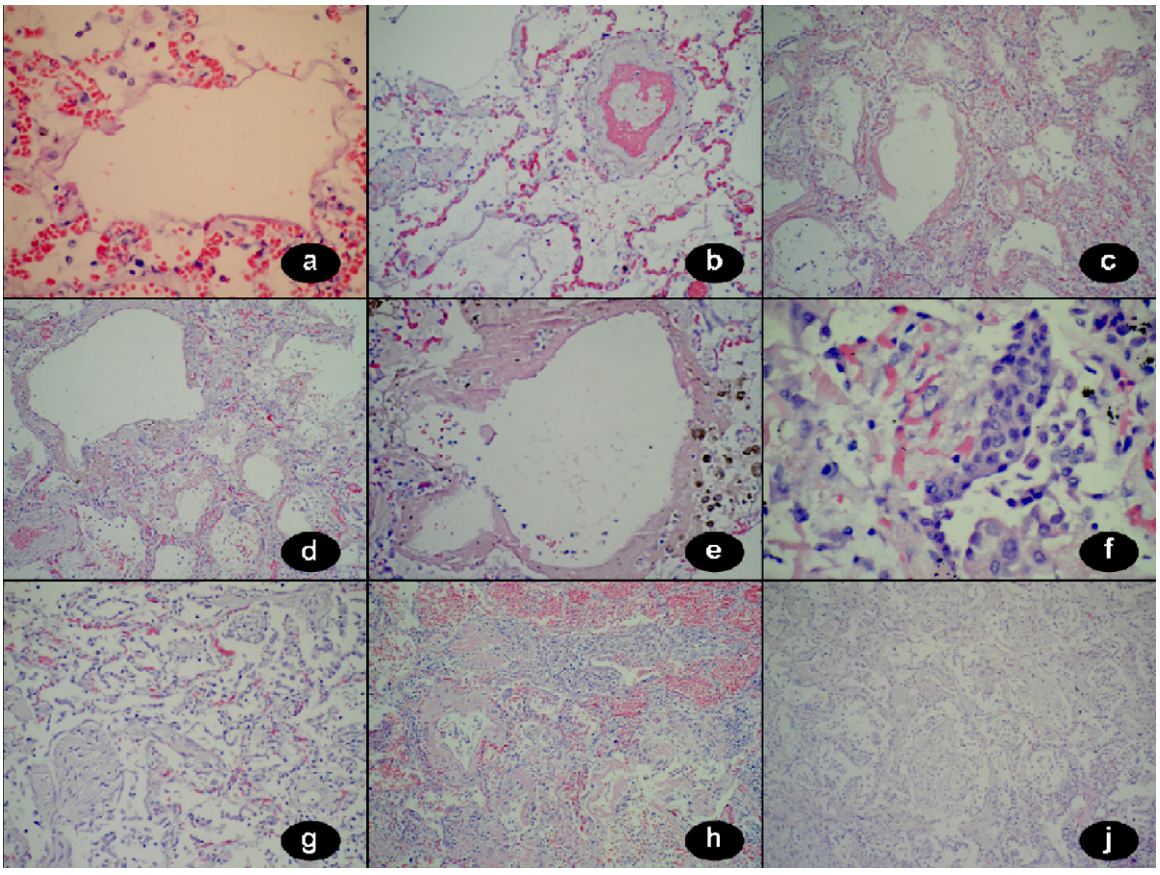

Fig. 1. (a–h, j) Representation of histological appearances (H&E stained) for lung tissue samples collected in this study. All these samples were representative of the spectrum of changes in ARDS, showing a clear disease progression from early stage leading to the end-stage lung fibrosis. The morphological description of these samples is shown in Table 1.

Table 2
The histological description for FFPE lung samples used in this study.

Patient	Sample	Stage	Grade	Autopsy description
I	A	Early	1	Alveolar walls with obvious congestion. Alveolar spaces with early membranes (refer Fig. 1a).
II	B	Early	2	Alveolar spaces with early membranes. Obvious bacterial overgrowth.
III	C	Early	3	Alveolar spaces with some inflammation and membranes. Early intravascular thrombus formation (refer Fig. 1b).
III	D	Early	4	Alveolar spaces with some inflammation and membranes (more than in previous). No intravascular thrombus formation.
IV	E	Early	5	Alveolar spaces with some inflammation and membranes (more than in previous). No intravascular thrombus formation (Fig. 1c).
IV	F	Early	6	Membranes (more than previously, Fig. 1d and e), giant cells (Fig. 1f) and vascular changes.
V	G	Late	7	Some areas relatively unaffected, other with BOOP-like appearance (Fig. 1g).
VI	H	Late	8.1	Intra-alveolar fibrosis and consolidation (Fig. 1h). Giant cells appearance.
VI	I	Late	8.2	Intra-alveolar fibrosis and consolidation, with giant cells. Early thrombus formation.
VII	J	Late	9	Extensive intra-alveolar fibrosis and consolidation. Early thrombus formation.
V	K	Late	10	Increased fibrosis and consolidation (refer Fig. 1j).
VII	L	Late	11	Fully established fibrosis and consolidation.

Table 3
List of genes that are over-expressed (mean expression level ≥1.5) in SARS-CoV infected lung tissue samples. All real-time qPCR results were expressed as fold changes in mRNA expression of patient samples with respect to the control samples and were normalized to the expression of the housekeeping gene β-actin.

No.	Over-expressed gene	Mean expression level for early stage	Mean expression level for late stage
1	BPI	159.68	11557.50
2	ACE2	387.16	2805.44
3	TAC1	1.04	765.88
4	CASP3	18.49	520.09
5	CEACAM8	13.67	274.43
6	DEFA4	41.77	147.51
7	IL10	9.37	121.10
8	CCL3	7.84	76.59
9	S100A8	2.38	73.41
10	HLA-A	1.22	60.59
11	PPBP	4.53	57.73
12	CCL27	1.00	49.40
13	LILRA3	6.50	43.80
14	MICB	16.79	38.89
15	ANPEP	2.74	36.04
16	MNDA	0.60	34.09
17	USP	8.94	32.79
18	ITGAM	4.88	32.36
19	CXCL9	49.52	30.22
20	IL1B	2.25	29.50
21	C1QB	4.68	28.38
22	ICAM1	4.56	26.57
23	MAD	10.93	26.33
24	CD69	1.96	25.76
25	CXCL10	164.93	25.57
26	IMPA2	4.50	24.09
27	IL1R1	3.22	21.94
28	GBP	132.93	21.58
29	CD68	1.31	18.48
30	EDN1	16.08	16.99
31	IL8	0.55	16.50
32	CSF2RA	0.45	16.47
33	CREBBP	5.98	16.35
34	FGF7	3.28	16.23
35	SMAD	8.83	15.34
36	MSR1	2.46	15.21
37	IL6	4.59	14.71
38	CD22	1.36	14.65
39	PECAM1	2.60	14.10
40	MALAT-1	4.15	12.27
41	BCAP29	7.14	11.87
42	ITGA2B	152.46	11.65
43	LILRA2	5.12	11.53
44	RAB31	1.32	11.13
45	B2M	5.28	10.93
46	AREG	2.17	9.79
47	RPGR	3.33	9.47
48	IFNA6	2.36	8.92
49	NFIL3	1.50	8.36
50	CD4	0.87	8.31
51	LTB4R	2.93	8.27
52	CCL28	4.10	8.14
53	VEGF	3.05	8.13
54	CXCL2	0.90	7.76
55	NFKBIA	2.93	7.57
56	IGF1	0.72	7.16
58	ATP1B1	1.74	7.06
59	NCF1	2.24	6.87
60	CASP9	0.33	6.75
61	KIAA0720	2.06	6.74
62	IRF3	0.73	6.71
63	CD14	0.83	6.70
64	TFPI	3.90	6.53
65	DTR	4.82	6.52
66	CD9	1.43	5.59
67	C4B	2.60	5.37
68	HIST2H2AA	2.69	5.06
69	SLPI	0.49	4.32
70	TNFSF5	1.73	4.00
71	CSF1	2.91	3.97
72	C3AR1	1.43	3.92
73	LTB	1.12	3.86
74	HLA-DRA	0.73	3.71
75	PTAFR	1.12	3.60
76	STAT1	9.86	3.43
77	ICAM2	1.84	3.41
78	C5R1	0.29	3.36
79	PIK3CB	1.65	3.33
80	TLR2	0.29	2.98
81	CD3Z	3.02	2.86
82	EGR1	0.94	2.72
83	CD8A	0.74	2.39
84	CCL2	2.16	2.31
85	TNFRSF1A	0.78	2.25
87	NR2F2	1.28	2.10
86	EGR2	1.22	2.10
88	IFNB1	0.82	1.75
89	IFNA1	2.08	1.52
90	HP	0.14	1.51
91	IFNG	1.74	1.05
92	CLC	12.29	1.00

(mean expression ≥1.5) in the disease samples versus the control samples (refer Table 3). We used Ingenuity Pathway Analysis to study the functionality of these over-expressed genes (refer Supplementary 2). From this list of 92 genes, the statistical analysis showed 26 genes significantly ($p < 0.05$) over-expressed and 5 genes significantly ($p < 0.05$) suppressed (refer Figs. 3 and 4, Table 4) in the progression of disease (early versus late disease stage).

As summarized in Table 4, the transcriptome of SARS-CoV infected patients in late disease stage was characterized by the high expression of genes coding for chemokine (IL-8), complement component (C1QB), antibacterial response protein (TLR2), cytokine receptor (IL1R1 and TNFSF5), apoptosis-related cystein protease (CASP3 and CASP9), immunoglobulin receptor family member (CD4 and CD14), growth factors (FGF7 and IFG1), transcription factors (IRF3 and NFIL3), major histocompatibility complex antigen (HLA-DRA), receptors (ANPEP, C5R1 and MSR1), protease (HP, USP33 and SLPI), cell adhesion molecule (CEACAM8) and genes of miscellaneous functions (BPI, CD68, MALAT-1, RAB31 and S100A8). In contrast, notably low expression levels of cytokine (CLC and CXCL10), cell adhesion molecule (ITGA2B), transcription factor (STAT1) and protease (GBP) were found in patients of late disease stage. Through the use of Ingenuity® Pathway Analysis, we demonstrated that the list of over-expressed genes were involved in immunological response (refer Fig. 5). Only a handful of genes appeared to be involved in this network analysis (with known and

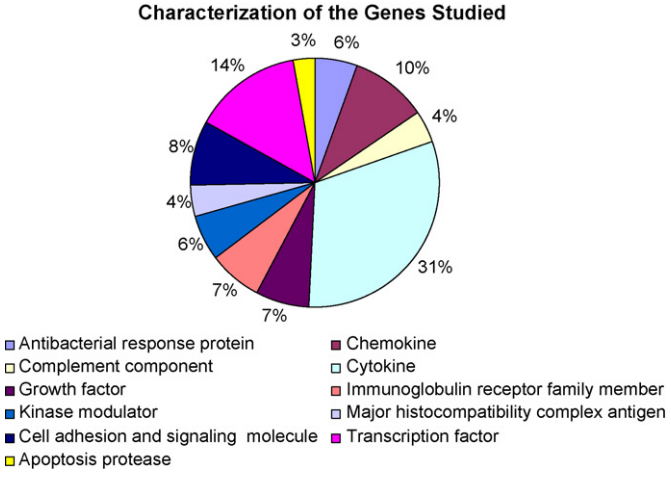

Fig. 2. The characterization of the list of 107 genes studied.

reported functionality), hence it highlights the novel insights in our study that majority of the over-expressed genes with important roles in the pathogenesis of SARS-CoV infection still remains unreported.

In order to confirm that the gene expression profiles have functional significance, we performed protein expression analysis by IHC for CD68, CD9 and PECAM. These were selected because they (a) were differentially expressed in both disease groups; (b) can be directly attributed to specific cellular types (macrophages, lymphocytic and endothelial); and (c) have robust, reported protocols used in the routine pathology setting and can be easily visualized and quantified. The results demonstrated that the gene expression profile correlates well with the degree of protein expression

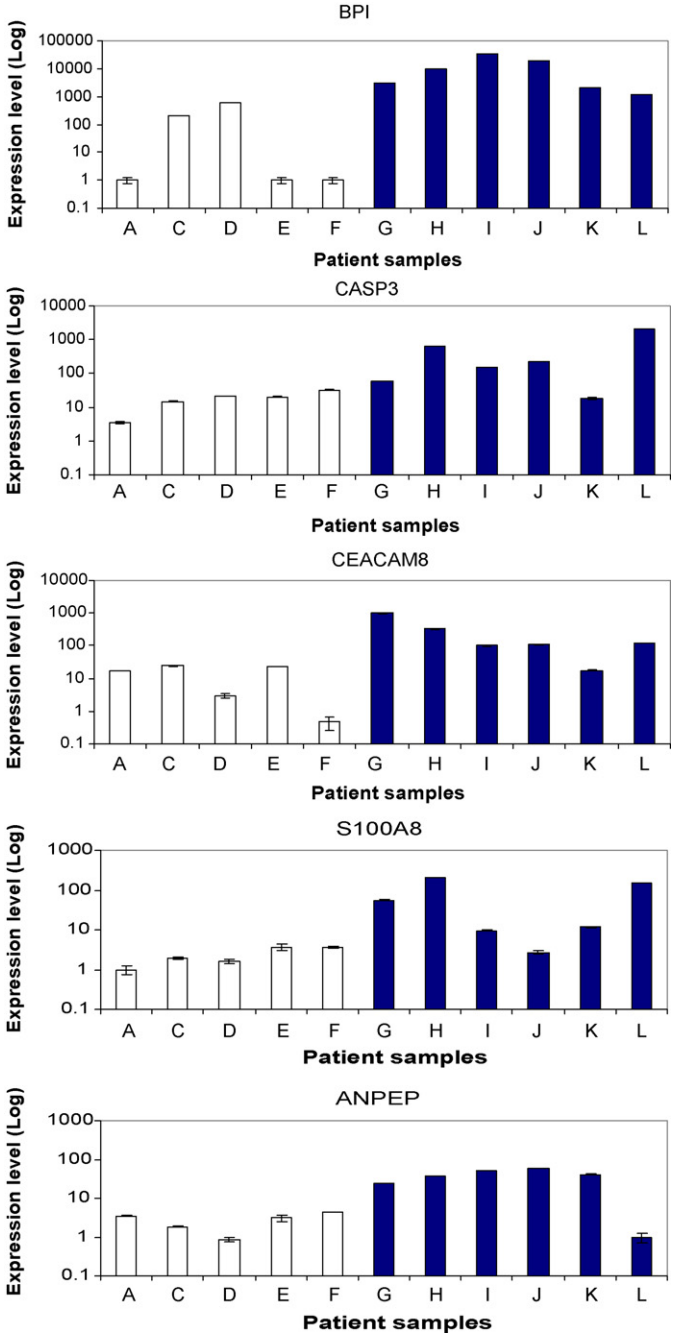

Fig. 3. Expression profiles of the top 5 genes that are significantly up-regulated in the severity progression of SARS-CoV infections (open bars represent early disease stage samples; filled bars represent late disease stage samples).

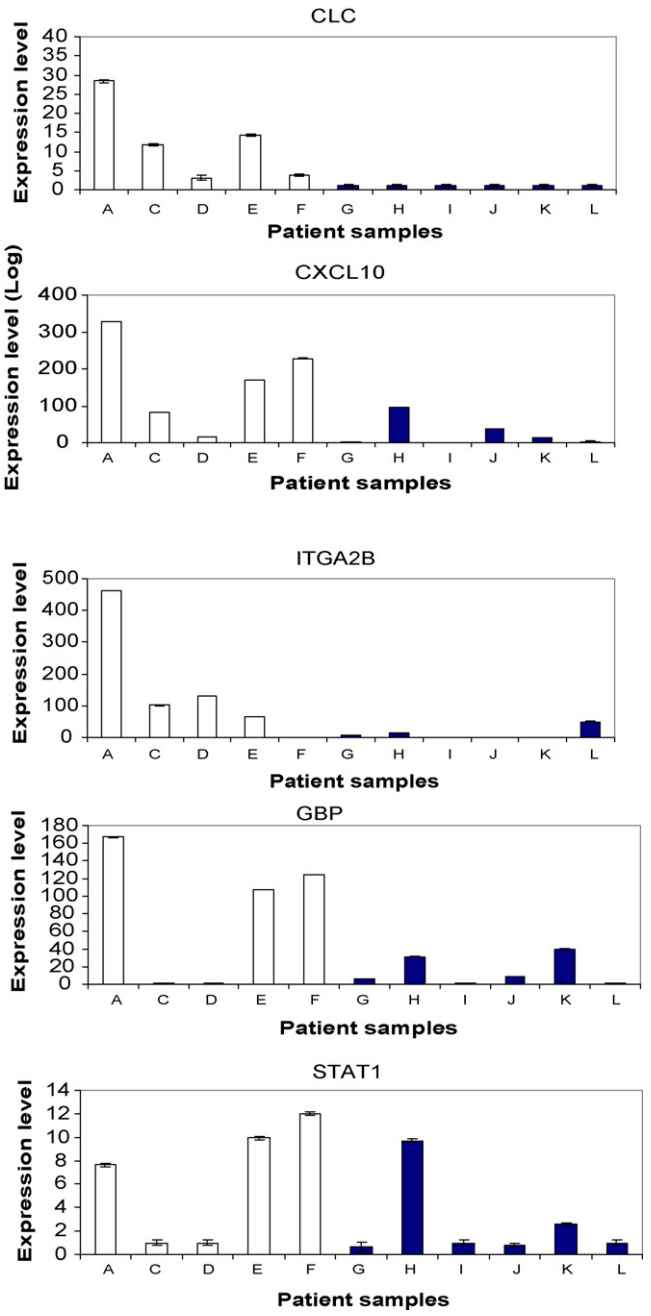

Fig. 4. Expression profiles of the top 5 genes that are significantly down-regulated in the severity progression of SARS-CoV infections (open bars represent early disease stage samples; filled bars represent late disease stage samples).

(refer Fig. 6). This highlighted the reliability of our gene expression profiling results.

4. Discussion

4.1. Characterization of gene expression profiles of SARS-CoV infections

The main contribution of our study is to establish which genes are of major biological and possibly clinical importance in a complex pathobiological reactions such as SARS-CoV infections and resulting ARDS. Here, we will discuss the roles and importance of the list of genes that are up- or down-regulated in the pathogenesis of ARDS in SARS-CoV infections.

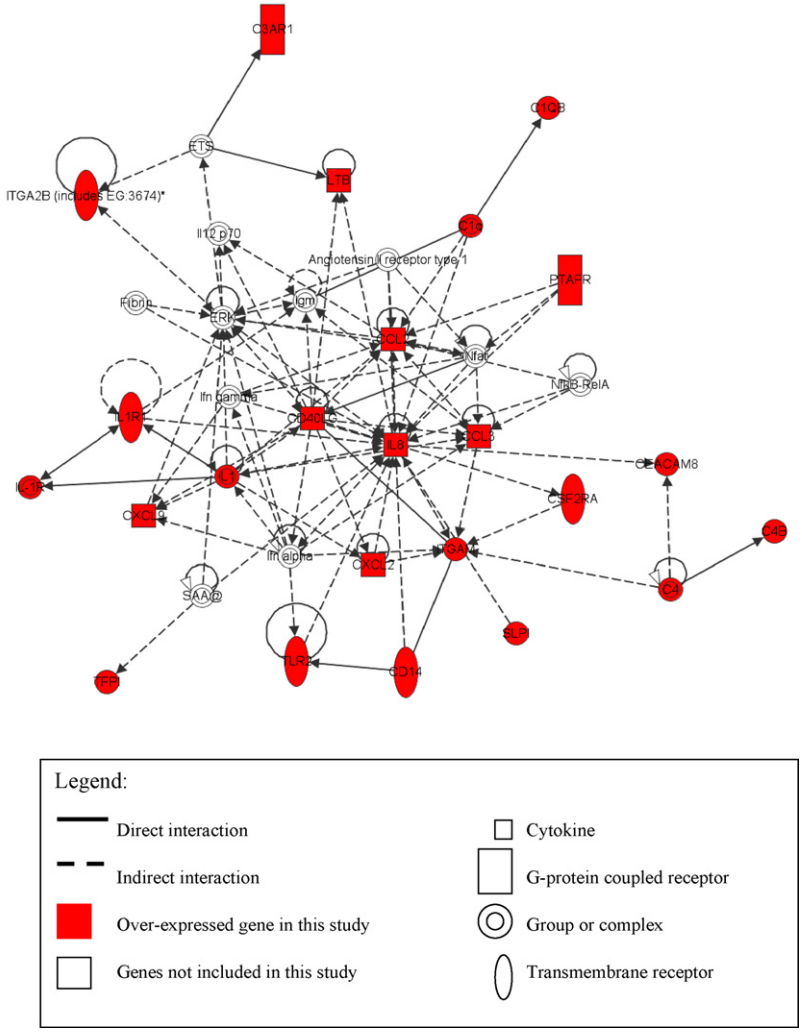

Fig. 5. List of genes involved in immunological response against viral or bacterial infection (data were analyzed through the use of Ingenuity® Pathway Analysis).

In our study, bactericidal/permeability-increasing protein (BPI) appears as the highest expressed gene in the late disease stage. It is a major constituent of neutrophils with anti-inflammatory properties and plays an integral part in innate immunity (Elsbach, 1998). Interleukin-8 (IL-8), another gene that is significantly over-expressed in disease samples, has been reported to cause airway inflammation and plays the role as neutrophilic activator in the pathogenesis of bronchiolitis. IL-8 has been also shown to up-regulate in the lung samples of SARS-CoV infected macaques (de Lang et al., 2007). Reports by Aichele et al. (2006) showed both BPI and IL-8 were released from neutrophils in a time-dependent manner following bacterial encounter in cystic fibrosis patients. In accordance to these studies, our data demonstrates up-regulation of BPI and IL-8 in SARS-CoV infections, presumably in an attempt to activate the immune response to combat the SARS-CoV infections.

Angiotensin converting enzyme 2 (ACE2) was identified as the functional cellular receptor for SAR-CoV and expressed at high level in the primary target cells of SARS-CoV (Li et al., 2003). We suggest that over-expression of ACE2 in our patient samples might correlate with increase susceptibility to SARS-CoV infection.

Tachykinin precursor 1 (TAC1) is present in sensory nerves of the lung. Reports indicated that TAC1 contributes to pathophysiology of bronchial hyper-responsiveness, airway construction, inflammation, chronic bronchitis and cough (Springer et al., 2005). Here, we show that over-expression of TAC1 contributes towards the appearance of the above-mentioned symptoms in SARS-CoV infected patients.

The key recognition receptors of the innate immune system are CD14 and Toll-like receptors (TLR). CD14 requires transmembrane receptors (e.g. TLRs) to initiate a stimulus-specific activation process. TLRs are responsible for quick recognition and response to pathogen, and consequently have vital roles in survival by boosting the host immune system during life-threatening infection (O'Neill, 2006). Here, we provide the evidence that innate immune response is activated in SARS-CoV infections.

Interferon regulatory factor-3 (IRF-3) is necessary for the transcriptional induction of IFN-stimulated genes (ISGs) in response to viral infection or TLR signaling (Cheng et al., 2006). Significant up-regulation of IRF-3 in response to SARS-CoV infection indicates that IRF-3 has distinct contributions to innate or acquired immunity via induction of ISGs.

Alanyl aminopeptidase (ANPEP) is a transmembrane protease present in leukocytes. It was identified as the cellular receptor for human coronavirus (Vijgen et al., 2004). Our findings strongly suggest that enrichment of ANPEP is a feature of late disease stage in SARS-CoV infection.

Tumor necrosis factor receptor superfamily, member 5 (TNFRSF5) is a key signaling molecule expressed by antigen-presenting cells of the immune system. Our detected TNFRSF5 up-regulations in SARS-CoV infection, may activate T cells and induce adhesion molecules such as carcino embryonic antigen

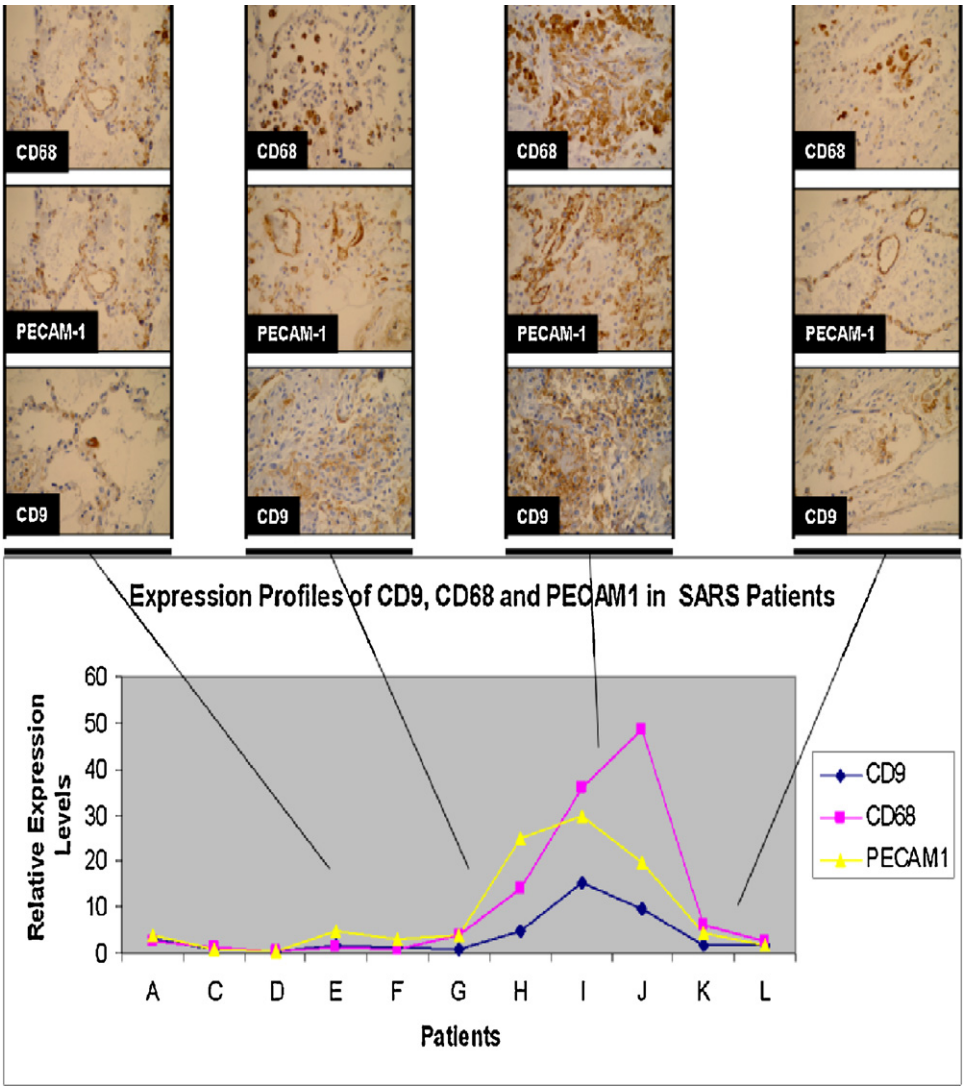

Fig. 6. The IHC results demonstrated the correlation between gene and protein expression profiles in SARS-CoV infected patients.

related cell adhesion molecule 8 (CEACAM8), which is expressed by activated monocytes and granulocytes to overcome the invading microorganisms (Deree et al., 2006), also up-regulated in our study.

Insulin-like growth factor-1 (IGF-1) has been reported to induce the hypoxia-inducible factor-α (HIF-α) and activates the hypoxic expression of target genes involved in cell adaptation to low oxygen concentrations (Fukuda et al., 2002). Macrophage scavenger receptor 1 (MSR1) is one of the hypoxia-induced genes that are involved in the clearance of pathogens and apoptotic cells (Platt et al., 1996). Haptoglobin (HP) is produced by inflammatory cells in protection against oxidative stress and inflammation (Eaton et al., 1982). Together, our observation on the up-regulation of IGF-1, MSR1 and HP demonstrate their roles in adapting the cells to the oxidative stress and hypoxic environment, another common occurrence in SARS-CoV infected patients.

Secretory leukocyte proteinase inhibitor (SLPI) is produced by lung tissues, as well as monocytes, alveolar macrophages and neutrophils. In ARDS, SLPI is markedly increased in bronchoalveolar lavage fluid and positively correlated with the multiple organ failure score (MOFS) (Sallenave et al., 1999; Asano et al., 1995). We reported increase of SLPI in SARS-CoV infected lung, this is consistent with the hypothesis that SLPI is the 'alarm inhibitor' at the onset of the inflammatory process.

S100 calcium binding protein A8 (S100A8) is present in the extracellular milleu during infections and inflammatory process. It has been shown to regulate monocyte, lymphocyte and neutrophil migration (Frosch et al., 2000). Our study also shows the Rab31 up-regulation in mediating the endocytosis and exocytosis responses. This is in concordance with the reports by Reghunathan et al. (2005).

CD68 is expressed in the endosomal compartment of all cells of mononuclear phagocyte lineage. Our CD68 gene up-regulatoin is a direct expression of monocyte recruitment and macrophages differentiation. This was confirmed by the CD68 protein up-regulation by IHC and the localization of its expression in the cytoplasmic compartment of macrophages.

Up-regulation of Fibroblast growth factor-7 (FGF-7) could be explained by its involvement in immune system modulation, as well as thrombin accumulation and fibrin deposition (Samoszuk et al., 2005). Integrin $\alpha_{IIb}\beta_3$ (ITGA2B) serves as the receptor for fibrinogen upon platelet stimulation. It is important in platelet adhesion and clot retraction (Calzada et al., 2002). We observe a significant up-regulation of ITGA2B at the early stage of the SARS-CoV infections, suggesting that upon SARS-CoV entry, ITGA2B was stimulated to mediate platelet aggregation and adhesion.

Cardiotrophin-like cytokine (CLC) has been reported to activate the proliferation of B cells and antibody production (Senaldi et

Table 4
SAM and Mann–Whitney analysis were performed to identify genes that are significantly up- or down-regulated in the progression of disease.

Gene	Mann–Whitney test		SAM test		Mean early expression level	Mean late expression level
	Z	p-val – 2 × 1 sided	Score(d)	q-Value (%)		
(a) Up-regulated						
BPI	−2.934	0.002	2.175	4.856	159.68	11557.50
CASP3	−2.082	0.041	N.A.	N.A.	18.49	520.09
CEACAM8	−2.562	0.009	1.794	4.856	13.67	274.43
S100A8	−2.082	0.041	1.845	4.856	2.38	73.41
ANPEP	−2.082	0.041	3.617	4.856	2.74	36.04
USP	N.A.	N.A.	0.884	0	8.94	32.79
C1QB	−1.761	0.093	1.999	4.856	4.68	28.38
IL1R1	−2.402	0.015	1.910	4.856	3.22	21.94
CD68	−2.562	0.009	2.130	4.856	1.31	18.48
IL8	−2.082	0.041	1.657	4.856	0.55	16.50
FGF7	−1.761	0.093	2.165	4.856	3.28	16.23
MSR1	−2.242	0.026	1.997	4.856	2.46	15.21
MALAT-1	N.A.	N.A.	1.061	0	4.15	12.27
RAB31	−2.082	0.041	2.403	4.856	1.32	11.13
NFIL3	−2.882	0.002	2.934	4.856	1.50	8.36
CD4	−2.402	0.015	2.578	4.856	0.87	8.31
IGF1	−2.882	0.002	4.448	4.856	0.72	7.16
CASP9	−2.242	0.026	1.768	4.856	0.33	6.75
IRF3	−2.882	0.002	2.635	4.856	0.73	6.71
CD14	−2.562	0.009	3.749	4.856	0.83	6.70
SLPI	−2.242	0.026	1.863	4.856	0.49	4.32
TNFSF5	N.A.	N.A.	0.884	0	1.73	4.00
HLA-DRA	−2.562	0.009	2.003	4.856	0.73	3.71
C5R1	−2.082	0.041	1.723	4.856	0.29	3.36
TLR2	−2.402	0.015	2.356	4.856	0.29	2.98
HP	−1.684	0.093	1.719	4.856	0.14	1.51
(b) Down-regulated						
CXCL10	2.402	0.015	N.A.	N.A.	164.93	25.57
GBP	N.A.	N.A.	−1.061	0	132.93	21.58
ITGA2B	2.201	0.026	N.A.	N.A.	152.46	11.65
STAT1	N.A.	N.A.	−0.884	0	9.86	3.43
CLC	3.077	0.002	N.A.	N.A.	12.29	1.00

Statistical significance: $p < 0.05$ by Mann–Whitney test; q-value < 5% by SAM method. N.A. = not available.

al., 2002). We have observed over-expression of CLC in the early stage of SARS-CoV infections, indicating that this may be the most important phase for B-cell related immunity.

Our results indicated that early stage of SARS-CoV infection has also induced the production of interferon-gamma-inducible protein 10 (CXCL10), a potent chemoattractant for activated T cells and natural killer (NK) cells (Vanguri and Farber, 1990), that can lead to leukocyte activation, extravasation and migration, thus generates a rapid innate antiviral response to aid the attempts of viral clearance in SARS-CoV infected lung.

GTPase guanylate-binding protein-1 (GBP-1) is a major IFN-γ-induced protein with anti-proliferative role in endothelial cells upon invasion by inflammatory cytokines (ICs). GBP-1 expression was inhibited in the progression of SARS-CoV infection. Thus, we propose that GBP-1 repression is important to restore the necessary neovascularization to accompany the late inflammatory changes in SARS-CoV related ARDS.

Signal transducer and activator of transcription 1 (STAT1) is important in transmitting inflammatory cytokine signals and inducing inflammatoty mediators from inflammatory cells. Phosphorylated STAT1 translocates transcription factors into the nucleus, where they activate IFN-inducible genes that participate in host defense (Levy and Darnell, 2002). We suggest that down-regulation of STAT1 increases the susceptibility of the host to SARS-CoV infection because of impaired IFN response.

4.2. Propose therapeutic targets in combating SARS-CoV infections

For most of the inflammatory mediators indicated in this study, a possible *in vitro* inhibitor has been postulated. For some of these genes there are already natural or synthetic inhibitors, and these may prove a useful starting point for future therapeutic design and prioritization of avenues for therapeutic intervention.

Natural and synthetic inhibitors of ANPEP, such as Bestatin, are able to influence immune functions and major biological events (cell proliferation, invasion, angiogenesis) (Bauvois and Dauzonne, 2006). C1qB is essential in recruiting the SARS-CoV to neutrophils, macrophages and T cells for phagocytosis. Treatment of all macrophages populations with dexamethasone resulted in a strong increase of C1q synthesis and secretion (Armbrust et al., 1997). Thus, Bestatin and dexamethasone could be a useful therapeutic agent, in combination with others, against SARS-CoV infection.

TAC receptor antagonists such as SR140333, SP142801 and SB223412 have been reported to demonstrate a significant broncho-protection role (Daoui et al., 2001) and could be a possible therapeutic target in the SARS disease.

Finally, airway inflammation is often associated with the infiltration of activated neutrophils and subsequent protease release; this can be prevented by the effect of SLPI to contain the excessive release of proteases. The specific site of synthesis (lung) with define functions make SLPI a very attractive candidate as potential therapeutic agent.

5. Conclusions

Only gene expression measurements that take place in the damaged tissues are likely to elucidate a complete physiopathological picture of the disease. Based on the evidence of our gene expression study, we hypothesize SARS-CoV infections require (i) expression of ANPEP, a receptor for CoV; (ii) impaired immune system by inhibiting STAT1 pathways and subsequently; (iii) prevent the production

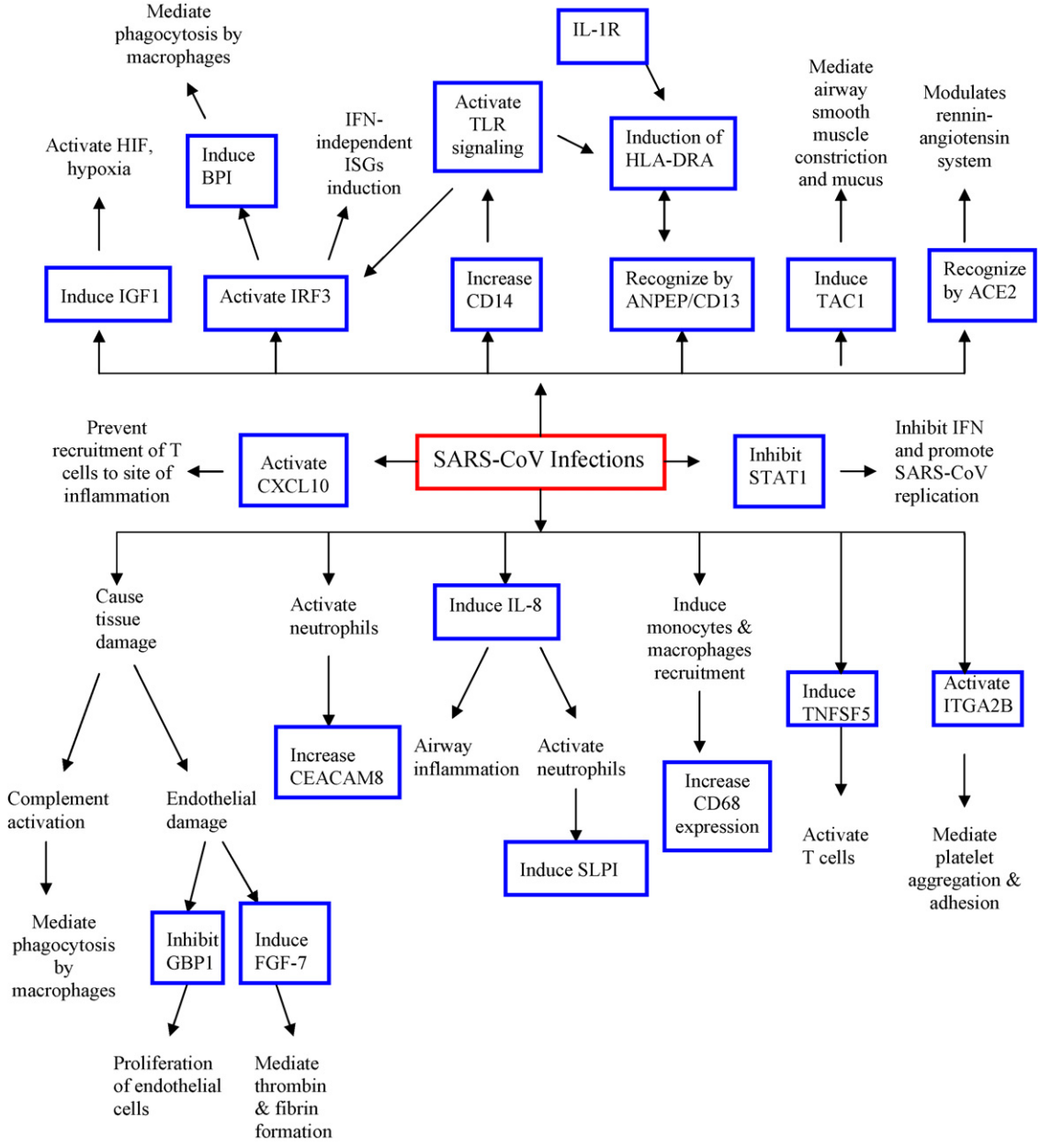

Fig. 7. Hypothesized pathogenesis model for SARS-CoV infections.

of IFNs. We hypothesize the model of SARS pathogenesis with new and novel insights in Fig. 7.

A complex immunological spectrum of changes such as the SARS-CoV related ARDS would involve numerous biological events related to neutrophilic activation, detection of SARS-CoV specific targets, cell migration, thrombosis and vascular proliferation, among others. Our study characterizes the main genes for these functions, and highlights the time in the disease development in which these biomarkers are of importance. Due to the limitation that collection of lung tissue collected from deceased patients and not in a time-point manner from the disease onset to the manifestation of SARS-CoV infection, we are unable to conclude if the expression profile explains exclusively the effects of the SARS-CoV itself, or the effects of other ongoing process at the tissue level such as the concomitant hypoxia, the cell infiltration which is a part of pathological process, or even the effects of therapeutic modalities used.

In conclusion, our study demonstrates that during the initial phase of the SARS-CoV infection, antiviral cytokines are suppressed. The affected lung tissue will then produce abundant chemokines and inflammatory cell recruitment. Parallel to this description, we describe the pathophysiology of the SARS-CoV related tissue changes and hypothesize the useful disease severity markers and therapeutic targets.

Acknowledgements

This work was supported by grant from the Biomedical Research Council (BMRC) and A*STAR (Agency for Science, Technology and Research), Singapore. We thank Dr. Jane Sohn Thomsen, Dr. Vladimir Andreevich Kuznetsov and Joshy George from Genome Institute of Singapore in support of this study.

Appendix A. Supplementary data

Supplementary data associated with this article can be found, in the online version, at doi:10.1016/j.virusres.2009.07.014.

References

Aichele, D., Schnare, M., Saake, M., Rollinghoff, M., Gessner, A., 2006. Expression and antimicrobial function of bactericidal permeability-increasing protein in cystic fibrosis patients. Infect. Immun. 74 (8), 4708–4714.

Armbrust, T., Nordmann, B., Kreibig, M., Ramadori, G., 1997. C1Q synthesis by tissue mononuclear phagocytes from normal and from damaged rat liver: up-regulation by dexamethasone, down-regulation by interferon gamma, and lipopolysaccharide. Hepatology 26, 98–106.

Asano, S., Kida, K., Koyama, T., Wada, H., Izawa, Y., Hosoda, K., Masuda, K., Suzuki, Y., 1995. A morphological study of lung secretory leukoprotease inhibitor in pneumonia. Am. J. Respir. Crit. Care Med. 151, 1576–1581.

Bauvois, B., Dauzonne, D., 2006. Aminopeptidase-N/CD13 inhibitors: chemistry, biological evaluations, and therapeutic prospects. Med. Res. Rev. 26 (1), 88–130.

Bhatia, M., Moochhala, S., 2004. Role of inflammatory mediators in the pathophysiology of acute respiratory distress syndrome. J. Pathol. 202, 145–156.

Calzada, M.J., Alvarez, M.V., Gonzalez-Rodríguez, J., 2002. Agonist-specific structural rearrangements of integrin $\alpha_{IIb}\beta_3$. J. Biol. Chem. 277, 39899–39908.

Cheng, T., Brzostek, S., Ando, O., Scoy, S.V., Kumar, K.P., Reich, N.C., 2006. Differential activation of IFN regulator factor (IRF)-3 and IRF-5 transcription factors during viral infection. J. Immunol. 176, 7462–7470.

Daoui, S., Ahnaou, A., Naline, E., Emonds-Alt, X., Lagente, V., 2001. Tachykinin NK_3 receptor agonists induced microvascular leakage hypersensitivity in the guinea-pig airways. Eur. J. Pharmacol. 433, 199–207.

de Lang, A., Baas, T., Teal, T., Leijten, L.M., Rain, B., Osterhaus, A.D., Haagmans, B.L., Katze, M.G., 2007. Functional genomics highlights differential induction of antiviral pathways in the lungs of SARS-CoV-infected macaques. PLoS Pathog. 3 (8), e112.

Deree, J., Lall, R., Melbostad, H., Grant, M., Hoyt, D.B., Coimbra, R., 2006. Neutrophil degranulation and the effects of phosphodiesterase inhibition. J. Surg. Res. 133, 22–28.

Ding, Y., He, L., Zhang, Q., Huang, Z., Che, X., Hou, J., Wang, H., Shen, H., Qiu, L., Li, Z., Geng, J., Cai, J., Han, H., Li, X., Kang, W., Weng, D., Liang, P., Jiang, S., 2004. Organ distribution of severe acute respiratory syndrome (SARS) associated coronavirus (SARS-CoV) in SARS patients: implications for pathogenesis and virus transmission pathways. J. Pathol. 203, 622–630.

Eaton, J.W., Brandt, P., Mahoney, J.R., Lee, J.T., 1982. Haptoglobin: a natural bacteriostat. Science 215, 691–693.

Elsbach, P., 1998. The bactericidal/permeability-increasing protein (BPI) in antibacterial host defense. J. Leuk. Biol. 64, 14–18.

Frosch, M., Strey, A., Vogl, T., Wulffraat, N.M., Kuis, W., Sunderkötter, C., Harms, E., Sorg, C., Roth, J., 2000. Myeloid-related proteins 8 and 14 are specifically secreted during interaction of phagocytes and activated endothelium and are useful markers for monitoring disease activity in pauciarticular-onset juvenile rheumatoid arthritis. Arthritis Rheum. 43, 628–637.

Fukuda, R., Hirota, K., Fan, F., Jung, Y.D., Ellis, L.M., Semenza, G.L., 2002. Insulin-like growth factor 1 induces hypoxia-inducible factor 1-mediated vascular endothelial growth factor expression, which is dependent on MAP kinase and phosphatidylinositol 3-kinase signaling in colon cancer cells. J. Biol. Chem. 277, 38205–38211.

Glass, W.G., Subbarao, K., Murphy, B., Murphy, P.M., 2004. Mechanisms of host defense following severe acute respiratory syndrome-coronavirus (SARS-CoV) pulmonary infection in mice. J. Immunol. 173, 4030–4039.

Ksiazek, T.G., Erdman, D., Goldsmmoth, C.S., Zaki, S.R., Peret, T., Emery, S., Tong, S., Urbani, C., Comer, J.A., Lim, W., Rollin, P.E., Dowell, S.F., Ling, A., Humphrey, C.D., Shieh, W., Guarner, J., Paddock, C.D., Rota, P., Fields, B., DeRisi, J., Yang, J., Cox, N., Hughes, J.M., LeDuc, J.W., Bellini, W.J., Anderson, L.J., SARS Working Group, 2003. A novel coronavirus associated with severe acute respiratory syndrome. N. Engl. J. Med. 348, 1953–1966.

Levy, D.E., Darnell, J.E.J., 2002. Stats: transcriptional control and biological impact. Nat. Rev. Mol. Cell Biol. 3, 651–662.

Li, W., Moore, M.J., Vasilieva, N., Sui, J., Wong, S.K., Berne, M.A., Somasundaran, M., Sullivan, J.L., Luzuriaga, K., Greenough, T.C., Choe, H., Farzan, M., 2003. Angiotensin-converting enzyme 2 is a functional receptor for the SARS coronavirus. Nature 426, 450–454.

Ng, P.C., Lam, C.W.K., Li, A.M., Wong, C.K., Cheng, F.W.T., 2004. Inflammatory cytokine profile in children with severe acute respiratory syndrome. Pediatrics 113, 7–14.

O'Neill, L.A.J., 2006. How toll-like receptors signal: what we know and what we don't know. Curr. Opin. Immunol. 18, 3–9.

Platt, N., Suzuki, H., Kurihara, Y., Kodama, T., Gordon, S., 1996. Role for the class A macrophage scavenger receptor in the phagocytosis of apoptotic thymocytes in vitro. Proc. Natl. Acad. Sci. U.S.A. 93, 12456–12460.

Reghunathan, R., Jayapal, M., Hsu, L.Y., Chng, H.H., Tai, D., Leung, B.P., Melendez, A.J., 2005. Expression profile of immune response genes in patients with severe acute respiratory syndrome. BMC Immunol. 6, 2.

Sallenave, J.M., Donnelly, S.C., Grant, I.S., Robertson, C., Gauldie, J., 1999. Secretory leukocyte proteinase inhibitor is preferentially increased in patients with acute respiratory distress syndrome. Eur. Respir. J. 13, 1029–1036.

Salto-Tellez, M., Tan, E., Lim, B., 2005. ARDS in SARS: cytokine mediators and treatment implications. Cytokine 29, 92–94.

Samoszuk, M., Kanakubo, E., Chan, J.K., 2005. Degranulating mast cells in fibrotic regions of human tumors and evidence that mast cell heparin interferes with the growth of tumor cells through a mechanism involving fibroblasts. BMC Cancer 5, 121.

Senaldi, G., Stolina, M., Guo, K., Faggioni, R., McCabe, S., Kaufman, S.A., Van, G., Xu, W., Fletcher, F.A., Boone, T., Chang, M., Sarmiento, U., Cattley, R.C., 2002. Regulatory effects of novel neurotrophin-1/b cell-stimulating factor-3 (cardiotrophin-like cytokine) on B cell function. J. Immunol. 168, 5690–5698.

Springer, J., Groneberg, D.A., Pregla, R., Fischer, A., 2005. Inflammatory cells as source of tachykinin-induces mucus secretion in chronic bronchitis. Regul. Pept. 124, 195–201.

Vanguri, P., Farber, J.M., 1990. Identification of CRG-2: an interferon-inducible mRNA predicted to encode a murine monokine. J. Biol. Chem. 265, 15049–15057.

Vijgen, L., Keyaerts, E., Zlateva, K., Van Ranst, M., 2004. Identifiation of 6 new polymorphisms in the human coronavirus 229E receptor gene. Int. J. Infect. Dis. 8, 217–222.

WHO, 2003. Summary of probable SARS cases with onset of illness from 1 November 2002 to 31 July 2003. Available: http://www.who.int.